5442 J. Med. Chem. 2009, 52, 5442–5448
DOI: 10.1021/jm900631m

Journal of Medicinal Chemistry Article

A Novel Decoy That Interrupts G93A-Superoxide Dismutase Gain of Interaction with Malate Dehydrogenase Improves Survival in an Amyotrophic Lateral Sclerosis Cell Model

Yael Mali and Nava Zisapel*

Department of Neurobiology, Tel Aviv University, Tel Aviv 69978, Israel

Received May 13, 2009

Human G93A-superoxide dismutase-1 (G93AhSOD1) mutation causes amyotrophic lateral sclerosis (ALS) in rodents and humans. Recent observations indicate gain of interaction of G93AhSOD1 with cytosolic malate dehydrogenase (MDH1) and subsequent impairment in the malate aspartate shuttle which is vital to neurons. Using fluorescence resonance energy transfer (FRET), we screened an MDH1 derived peptide library for a decoy that would interrupt the G93AhSOD1−MDH1 interaction. A specific 23 amino acid blocker of this interaction was thus discovered, and interruption of interaction was confirmed by pull-down immunoprecipitation studies. A cell permeable 5-carboxytetramethylrhodamine derivative of the decoy peptide improved ATP content of motor neuron derived NSC-34 cells expressing G93AhSOD1 and enhanced cell survival under rotenone and low glucose challenges. Decoy agents capable of interrupting the gain of toxic interaction of G93AhSOD1 with MDH1 provide further evidence for the role of malate aspartate shuttle inhibition in G93AhSOD1 toxicity and a promising new route in ALS drug research.

Amyotrophic lateral sclerosis (ALS[a]) is a neurodegenerative disorder affecting motor neurons in the brain and spinal cord. In 3% of all ALS cases the disease is caused by mutation in the human Cu/Zn superoxide dismutase (hSOD1) gene. The neurodegenerative disorder is due to gain of toxic function rather than loss of hSOD1 enzymatic activity.[1−6] We have recently identified, using a fluorescence resonance energy transfer (FRET) based screening system and pull-down immunoprecipitation, "gain-of-interaction" of the ALS-linked G93AhSOD1 mutant with cytosolic malate dehydrogenase (MDH1).[7] Studies in symptomatic transgenic mice expressing a mutant SOD1(Leu126delTT) have also revealed interaction of the disease causing gene product with cytosolic malate dehydrogenase in the spinal cord.[8] MDH1 is part of the malate aspartate shuttle, controlling brain mitochondrial NADH/NAD$^+$ balance. Impairments in this shuttle may enforce anaerobic metabolism, particularly damaging to neurons.[9] Cells expressing the mutant protein are more vulnerable to inhibition of the electron transport chain in mitochondria by rotenone and, consistent with inhibition of the malate−aspartate shuttle, have low ATP levels compared to wild-type (WT) hSOD1 expressing cells.[10,11] It was thus hypothesized that certain MDH1 derived peptides comprising the interacting motif would compete with MDH1 for the G93AhSOD1−MDH1 interaction site (decoy) and would consequently interrupt the G93AhSOD1−MDH1 interaction. If the interaction does indeed play a major role in the G93AhSOD1 gain of toxic interactions, such decoy peptide should alleviate mutant hSOD1 toxicity.

A fluorescence resonance energy transfer (FRET) based system[12] was thus designed to screen for agents that would interrupt the "gain-of-interactions" between the G93AhSOD1 and MDH1 in live cells. Thus, NSC-34 cells were co-transfected with a myc-tagged cDNA library constructed from mouse MDH1 derived fragments, cyan fluorescence protein tagged G93AhSOD1 (G93AhSOD1-CFP) and yellow fluorescence protein tagged MDH1 (MDH1-YFP) expression plasmids. Proximity was assessed by FRET efficiency between the CFP (donor) and YFP (acceptor) in live NSC-34 cells. FRET was evidenced by fluorescence emission of YFP tagged MDH1 following excitation of the CFP tagged G93AhSOD1. In the case of a decoy that interrupted the G93AhSOD1−MDH1 interaction, the FRET would be diminished and excitation of the CFP and YFP tagged proteins would result in fluorescence emission at their respective wavelengths. Using this method, we discovered a specific 23 amino acids "decoy" peptide that impaired the G93AhSOD1-CFP/MDH1-YFP interaction. Further immunoprecipitation studies confirmed the interruption of the interaction by this decoy. The functional significance of the loss of such interaction was assessed by alleviation of rotenone toxicity, survival under low glucose conditions, and cell ATP levels in NSC-34 cells expressing the G93AhSOD1 protein.

Results

Identification of Potential G93AhSOD1-CFP/MDH1-YFP Interaction Inhibitors. A Myc tagged peptide library expressing small fragments of the MDH1 was prepared. G93AhSOD1-CFP and MDH1-YFP expression plasmids

*To whom correspondence should be addressed. Phone: +972-3-6409611. Fax: +972-3-6407643. E-mail: navazis@post.tau.ac.il.

[a] Abbreviations: ALS, amyotrophic lateral sclerosis; CFP, cyan fluorescence protein ; FRET, fluorescence resonance energy transfer; GFP, green fluorescence protein; hSOD1, human superoxide dismutase-1; MDH1, cytosolic malate dehydrogenase; WT, wild-type; YFP, yellow fluorescence protein; TAMRA, 5-carboxytetramethylrhodamine.

 Published on Web 08/11/2009

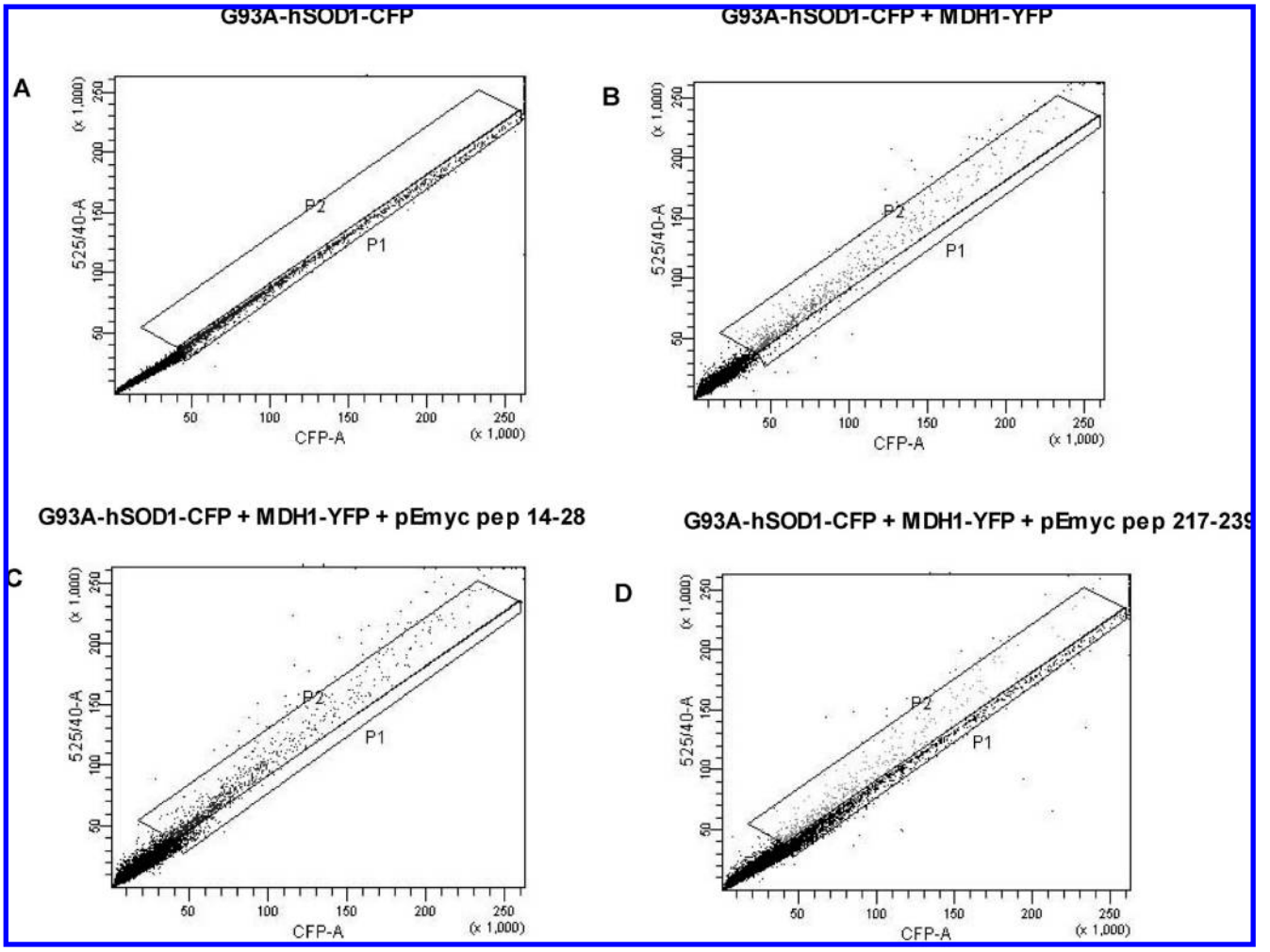

Figure 1. FACS analysis of FRET positive and negative cells. NSC-34 cells were transfected with G93AhSOD1-CFP expression plasmid and (A) control myc plasmid, (B) MDH1-YFP expression plasmid and control myc plasmid, (C) MDH1-YFP expression plasmid and myc-tagged plasmid containing MDH1 residues 14−28, (D) MDH1-YFP expression plasmid and myc-tagged plasmid containing MDH1 residues 217−239. The characteristic fluorescence patterns of individual cells (represented by dots) are depicted. Cells associated with the gating areas P1 are FRET negative (showing no YFP emission upon CFP excitation), whereas those associated with P2 are FRET positive (in which CFP excitation triggers YFP emission).

were co-transfected into NSC-34 cells with and without the myc-tagged library and the cells subjected to fluorescence activated cell sorting (FACS; excitation 425 nm (CFP), emission 525/540 nm (YFP)). The FRET based screening of the myc-tagged MDH1 fragment library for potential inhibition of G93AhSOD1-CFP/MDH1-YFP interaction is presented in Figure 1. The gating area denoted P1 is associated with FRET negative cells (showing no YFP emission upon CFP excitation), whereas the gating area denoting P2 is associated with FRET positive cells.[12] Cells transfected with G93AhSOD1-CFP expression plasmid alone were FRET negative and found exclusively in P1 gating area (Figure 1A). The majority of NSC-34 cells co-transfected with G93AhSOD1-CFP/MDH1-YFP and the control expression vector were associated with the P2 (FRET positive) gating area (Figure 1B). In cells co-transfected with G93AhSOD1-CFP/MDH1-YFP and the MDH1 expression library there was a 5-fold increase in cells associated with the P1 (FRET negative) gating area than in the presence of the control expression vector. The FRET negative G93AhSOD1-CFP/MDH1-YFP transfected cells (P1 gating area) were sorted out, and RNA was extracted, converted into cDNA, and cloned for identification of the inserts' DNA sequences. As can be seen in Table 1, in half (16 of 32) of the analyzed clones the insert sequence was identified as nucleotides 748−814 of the MDH1 cDNA which corresponds to a 23 amino acid residues sequence (217−239) in the MDH1 protein. In 10 of the 32 clones the insert sequence was identified as nucleotides 135−181 of the MDH1 cDNA which corresponds to a 14 amino acid residues sequence (14−28). In four clones, the insert sequence corresponded to nucleotides 1054−971 (inverted sequence) and in two to a longer sequence (nucleotides 537−747) corresponding to MDH1 amino acids 147−215.

The clones that expressed open reading frames of the identified MDH1 fragment sequences were used for further validation of their ability to interrupt the G93AhSOD1-CFP/MDH1-YFP interaction (Figure 1C,D). Co-transfection of NSC-34 cells with G93AhSOD1-CFP and MDH1-YFP and the cDNA clone corresponding to MDH1 amino acid residues 14−28 (Figure 1C) and 147−215 (data not shown) did not interrupt the G93AhSOD1-CFP/MDH1-YFP interaction, and most cells were associated with the P2 (FRET positive) area. As can be seen in Figure 1D, co-transfection of NSC-34 cells with G93AhSOD1-CFP and

Table 1. Decoy Peptide Candidates

nucleotide	amino acid	no. of clones	remarks
748−814	217−239	16	
135−181	14−28	10	
1054−971		4	inverted sequence
537−747	147−215	2	
total clones		32	

MDH1-YFP and the cDNA clone corresponding to MDH1 amino acid residues 217−239 resulted in 79% of the cells associated with P1 (FRET negative) rather than with P2.

Confirmation of G93AhSOD1-CFP/MDH1-YFP Interaction Inhibition. The fragment corresponding to MDH1 residues 217−239 (decoy peptide) was synthesized and labeled with 5-carboxytetramethylrhodamine (TAMRA) dye (N-TAMRA-SWLKGEFITTVQQRGAAVIKARK; TAMRA-decoy peptide). A TAMRA labeled peptide corresponding to nuclear localization signal (N-TAMRA-PKKKRKV; TAMRA-NLS peptide) was also prepared and used as nondecoy control. The cell permeability of the TAMRA-labeled peptides was assessed by fluorescence confocal microscopy following incubation of the NSC-34 cells with 1 μM of the respective TAMRA labeled peptides for 24 h. Figure 2A shows the intracellular localization of the TAMRA decoy and the control TAMRA-NLS peptides in the NSC-34 cells. Both peptide derivatives penetrated 100% of the cells. However, while the TAMRA-NLS peptide was distributed in the cell cytoplasm, the TAMRA-decoy peptide was localized both in the cytoplasm and in clustered structures. Colocalization studies indicated that the TAMRA-decoy peptide was not associated with the mitochondria or lysosomes (Figure 2B). Some of the decoy peptide clusters colocalized with early endosomes, but the majority colocalized with G93AhSOD1 (Figure 2B).

Pull-down immunoprecipitation studies were then performed in NSC-34 cells co-transfected with G93AhSOD1 or WThSOD1 and MDH1-YFP expression plasmids.

As shown in Figure 3 (lanes 1 and 2), in cells treated with vehicle or TAMRA-NLS peptide immunoprecipitation of G93AhSOD1 resulted in coprecipitation of MDH1 whereas in cells treated with the TAMRA-decoy peptide MDH1 was not pulled down with the anti-G93ASOD1 antibody (Figure 3, lane 3). Similarly, immunoprecipitation of WThSOD1 which does not interact with MDH1 did not result in coprecipitation of MDH1 (Figure 3, lane 4).

Structural Considerations of the G93AhSOD1/MDH1 Interacting Motif. Figure 4A shows a putative Patchdock algorithm-derived structure for the SOD1/MDH1 complex. As can be seen, the sequence corresponding to the decoy peptide (in red) is localized at the MDH1 surface facing SOD1, thus forming a putative interaction motif between the hSOD1 mutant and MDH1. Following the report of Watanabe et al.[8] on a monomeric form of ALS-related hSOD1 mutant, we have further applied the Patchdock algorithm to predict a possible interaction orientation between MDH1 (PDB code 5MDH) and monomeric SOD1 (PDB code 1kmg). This analysis predicted a similar orientation for MDH1 and the monomeric as for the dimeric hSOD1 mutant (Figure 4B). Here too, the decoy peptide sequence is proximal to hSOD1 surface (~10 nm distance).

ATP Levels in NSC-34 Cells Expressing the G93AhSOD1 Protein and the Effects of the Decoy Peptide on Them. Figure 5 presents the ATP levels in NSC-34 cells stably expressing the inducible forms of GFP tagged G93AhSOD1 and

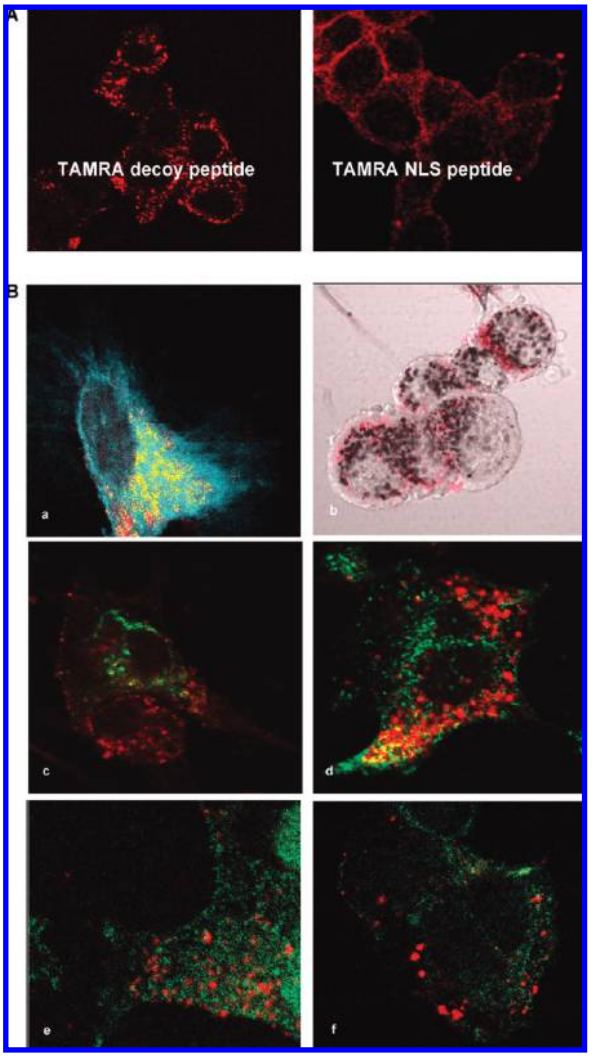

Figure 2. Confocal microscopy analysis of decoy peptide localization. (A) Confocal fluorescence microscopy of NSC-34 cells incubated with TAMRA tagged decoy MDH1 derived peptide corresponding to the 23 amino acid residues 217−239 sequence (left panel) and TAMRA tagged NLS (nuclear localization sequence) peptide (right panel). (B) Superimposed confocal microscopy images of TAMRA tagged decoy peptide (red) and (a) G93AhSOD1-CFP, (b) MTT (mitochondrial marker), (c) RUB-5-GFP (early endosomes marker), (d) Oregon green labeled transferrin (endosomal marker), (e) cathepsin D (lysosomal marker), (f) Lamp1 (lysosomal marker). Colocalization is indicated by yellow color in the images.

WThSOD1 proteins. ATP levels in the G93AhSOD1 cells were lower by 30% than in the WThSOD1 cells (Figure 5A). Incubation of the G93AhSOD1 cells with the TAMRA-decoy peptide significantly increased ATP levels to 90% of those found in the WThSOD1 cells and WThSOD1 cells incubated with TAMRA-NLS control peptide (Figure 5B).

Effect of Rotenone and Low Glucose on G93AhSOD1 Cells Survival. The effects of rotenone on cell survival was assessed in stable cell lines expressing the inducible forms of G93AhSOD1-GFP and WThSOD1-GFP. As seen in Figure 6A, incubation of the mutant G93AhSOD1-GFP expressing cells with the rotenone for 24 h reduced survival by 20% compared to WThSOD1-GFP under these consitions. The TAMRA-decoy peptide significantly protected the G93AhSOD1-GFP cells against rotenone toxicity, and survival

increased to 98% of that of the rotenone treated WThSOD1 expressing cells (Figure 6A). The TAMRA-NLS control peptide did not have any effect (data not shown).

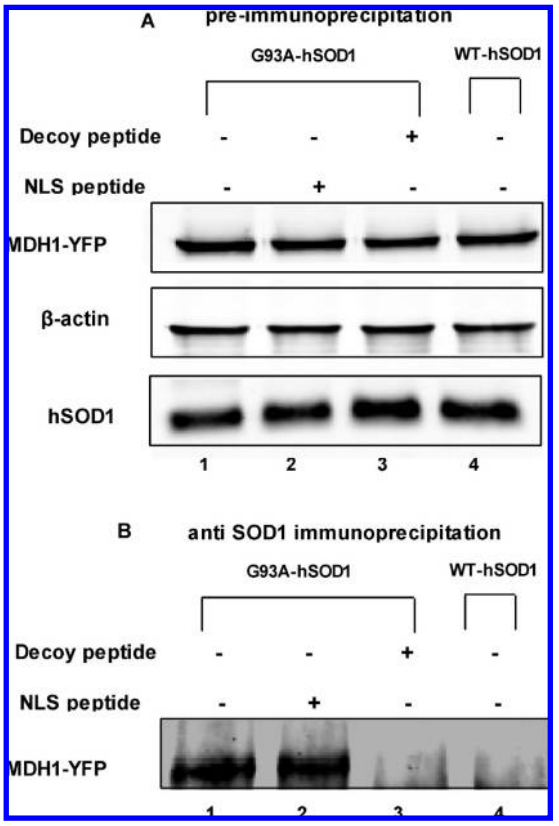

Figure 3. Pull-down immunoprecipitation of G93AhSOD1 and cytMDH in the absence and presence of the decoy peptide corresponding to the MDH1 residues 217−239. NSC-34 cells were co-transfected with YFP-MDH1 and untagged G93A-hSOD1 and incubated with (1) 0.02% acetic acid vehicle, (2) TAMRA labeled NLS peptide, (3) TAMRA labeled decoy peptide corresponding to MDH1 residues 217−239. In (4) NSC-34 cells were co-transfected with YFP-MDH1 and untagged WT-hSOD1. Then 48 h later cells were lysed and subjected to immunoprecipitation with anti-hSOD1 antibodies and Western blot analyses: (A) YFP-MDH1, actin and hSOD1 preimmunoprecipitation and (B) YFP-MDH1 in the immunoprecipitated fractions.

The effects of low glucose (2 mg/mL) on cell survival were also assessed in stable cell lines expressing the inducible forms of G93AhSOD1-GFP and WThSOD1-GFP. As seen in Figure 6B, incubation of the G93AhSOD1 expressing cells in low glucose for 24 h reduced survival of G93AhSOD1-GFP cells by 20% compared to WThSOD1-GFP under these conditions. Incubation of the G93AhSOD1 expressing cells with the TAMRA-decoy peptide significantly protected the cells against low glucose, and cell survival was 97% of that of the low glucose treated WThSOD1 expressing cells (Figure 6B). The TAMRA-NLS control peptide did not have any effect (data not shown).

Discussion

A novel FRET based screening system was designed in live motor-neuron derived cells to identify agent(s) that can interrupt the gain of interaction between mutant hSOD1 and MDH1. Pull-down immunoprecipitation studies confirmed that a cell permeable TAMRA labeled derivative of the decoy peptide thus identified interrupts the interaction between MDH1-YFP and untagged mutant hSOD1.

The sequence corresponding to the identified MDH1 derived peptide is located at the surface of MDH1 that is predictably part of the putative G93AhSOD1/MDH1 interaction motif. The peptide may thus act as a decoy and compete with MDH1 for G93AhSOD1 binding. Clearly, the structural analysis shows that the distance between the hSOD1 and MDH1 at the putative interaction site, although in proximity (∼10 nm) to the hSOD1 surface, is too large for actual binding. In this respect it is important to note that none of the available crystal structures show clear evidence for structural differences between ALS-linked hSOD1 mutants and WThSOD1. A plausible assumption is that the formation of the crystal may impinge on the representation of some less favorable conformations that exist in solution. The predicted distances derived from the available crystal structures may thus differ from the distances in solution in which the two interacting proteins might form a closer alignment.

MDH1 activity is highly influenced by repulsion in surface-charged residues.[13] The interaction site, at the MDH1 surface, may thus influence electrostatic interactions that contribute

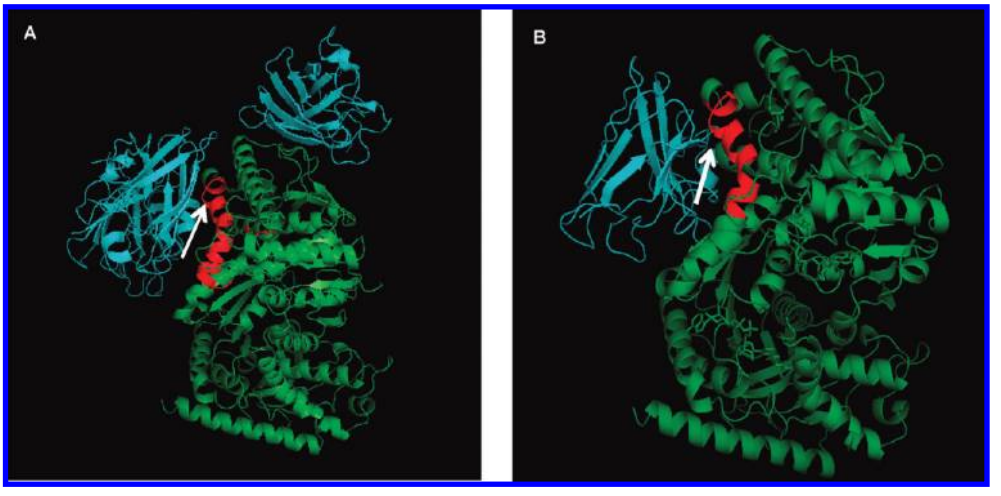

Figure 4. Patchdock molecular docking algorithm derived prediction of the mutant hSOD1/MDH1 complex. (A) MDH1 (PDB code 5MDH) with the ALS-associated human copper−zinc superoxide dismutase (CuZnSOD) mutant D125H (PDB code 1p1v). (B) MDH1 (PDB code 5MDH) with the monomeric form of mutant SOD1 (PDB code 1kmg). SOD1 is presented in blue, MDH in green, and the MDH1 217−239 sequence in red. Area of potential interaction between MDH1 and SOD1 is denoted by an arrow.

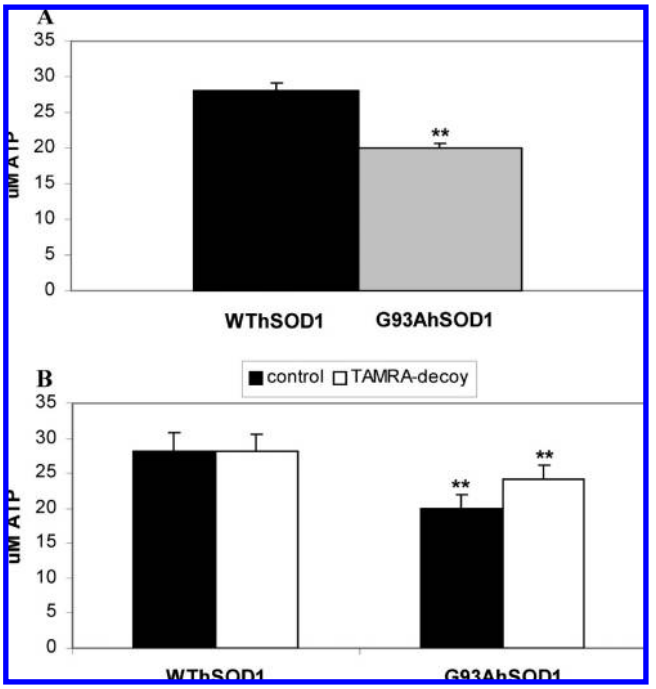

Figure 5. ATP levels in G93AhSOD1 and WThSOD1 cells and the effects of the decoy peptide on them. (A) ATP levels in G93AhSOD1-GFP compared to WThSOD1-GFP expressing cells. (B) ATP levels in WThSOD1-GFP treated with TAMRA labeled NLS peptide (black bar), G93A-hSOD1 cells treated with TAMRA labeled NLS peptide (gray bar), and G93A-hSOD1 cells treated with TAMRA labeled decoy peptide corresponding to MDH1 residues 217−239 (blank bar). Results are the mean of three experiments in octaplicates: (**) significant difference ($p < 0.01$; t test) between WThSOD1-GFP and G93AhSOD1-GFP ATP levels and between TAMRA decoy and NLS peptides treated cells.

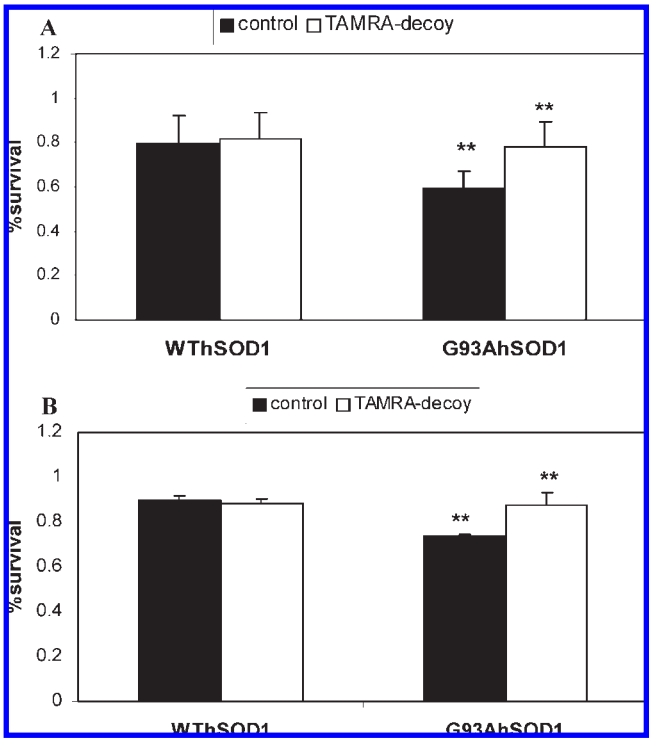

Figure 6. Effects of rotenone and low glucose levels on survival of G93AhSOD1 cells and the effects of the decoy peptide. (A) WThSOD1-GFP (black bar) and G93ASOD1GFP (gray and blank bars) NSC-34 cells were incubated with doxycycline (1 μg/mL) and treated with 2 μM rotenone in the presence of vehicle (black and gray bars) or 1 μM TAMRA labeled decoy peptide corresponding to MDH1 residues 217−239 (blank bars) for 48 h. (B) WThSOD1-GFP (black bar) and G93AhSOD1-GFP (gray and blank bars) NSC-34 cells were incubated with doxycycline (1 μg/mL) and treated with low (2 mg/mL) glucose in the presence of vehicle (black and gray bars) or 1 μM TAMRA labeled decoy peptide corresponding to MDH1 residues 217−239 (blank bars) for 48 h. Cell viability was assessed by methylene blue assay: (**) significant difference ($p < 0.01$; t test) between WThSOD1-GFP and G93AhSOD1-GFP cells and between peptide and vehicle treated G93ASOD1-GFP cells. Results are expressed as % of survival of the respective cell types without challenge.

significantly to the stability of MDH1 active conformation. MDH1 inhibition diverts neurons toward anaerobic metabolism.[7] The lower energy yield of anaerobic metabolism may explain the lower ATP content of G93AhSOD1 cells. Indeed, lower ATP production has recently been observed in cells that were treated with malate aspartate shuttle inhibitors.[14] A 30% reduction in ATP levels has previously been noted in cell lines expressing the mutant G93AhSOD1 compared to WThSOD1 expressing cells.[11] Furthermore, transgenic mice expressing G93AhSOD1 exhibit almost 50% reduction in ATP 30 days before ALS symptoms onset.[15] Compatible with these studies, expression of the G93AhSOD1-GFP in the NSC-34 cells reduced ATP production by 30% compared to WThSOD1-GFP cells. The release of MDH1 from the interaction with hSOD1 would predictably allow its full enzymatic activity. Indeed, with the decoy peptide, the energetic state of the G93AhSOD1 cells improved as evidenced by recovery of cell ATP to close to control WThSOD1 levels.

The greater vulnerability of G93AhSOD1 cells to rotenone is compatible with impairments in mitochondrial function which is evident in ALS animal and cell models.[16−18] The observation that a decoy peptide which interrupts the G93AhSOD1/MDH1 interaction also rescues the cells against rotenone toxicity seems to imply that the damage to the mitochondrial functioning seen in the G93AhSOD1 ALS models is indeed related to the malate aspartate shuttle impairment. Enhanced glucose exploitation through glycolysis is another hallmark of malate aspartate shuttle inhibition because mitochondrial ATP production is attenuated because of impaired NAD^+/NADH balance.[14] As shown in this study, the G93AhSOD1 expressing cells are indeed more vulnerable to low glucose than WThSOD1 cells. Evidently, the decoy peptide ameliorates the toxic gain of function of the mutant hSOD1, as in its presence the cells expressing the ALS-linked protein were less vulnerable to rotenone toxicity and low glucose than in its absence.

The ability of the decoy peptide to improve survival and energetic state of the G93AhSOD1 cells to levels comparable to those of the WThSOD1 cells is compatible with the notion that the gain of interaction of the G93AhSOD1 with MDH1 is a major component of mutant hSOD1 toxicity.

It is interesting to note that whereas ATP levels in the TAMRA-decoy peptide treated G93AhSOD1 cells is still somewhat lower (by 10%) than WThSOD1 cells, the survival rates under rotenone challenge are similar. This suggests a certain tolerance to a limited decrease in ATP production. Indeed, in Fanconi anemia cell lines FANCA and FANCC challenged with rhodamine-1,2,3, which impairs the efficiency of electron transport and consequently the respiratory chain and oxidative phosphorylation, reduction in ATP production

to 90% (FANCA cells) and even 75% (FANCC cells) had no effect of survival.[19]

In conclusion, our results demonstrate a feasible approach to the identification of agents that interrupt the "gain of interaction" between mutant SOD1 and MDH1. The decoy peptide thus identified may provide insights into the interaction motifs. The ability of the decoy peptide to reverse at least in part some of the toxic effects of the mutant hSOD1 may provide insights into the pivotal role of the G93AhSOD1/MDH1 interaction in neuronal vulnerability to challenge impaired energy production and subsequently degeneration in ALS. The finding of an agent that interrupts the G93AhSOD1/MDH1 protein interaction may thus have major implications on future ALS drug development.

Experimental Section

Materials. Dulbecco's modified Earle's medium (DMEM), heat inactivated fetal calf serum (FCS), L-glutamine, penicillin streptomycin, and EZ-first strand cDNA synthesis kit were obtained from Biological Industries (Beit Haemek, Israel). Celltiter-Glo luminescent cell viability assay and ATP quantification kits were from Promega Corporation, doxycycline, rotenone, and methylene blue were from Sigma-Aldrich (St. Louis, MO), transIT-LT1 transfection reagent was from MIRUS, protein A-Sepharose was from Amersham Bioscience (Sweden), and ampicillin was from Applichem (Germany). Polyclonal (rabbit) antihuman SOD1 and polyclonal (rabbit) anti-Lamp1 antibodies were purchased from Santa Cruz, Inc. (Santa Cruz, CA). Polyclonal (rabbit) anti-GFP was from Abcam (U.K.), goat antirabbit-IRDey-800 was from Li-Cor (Lincoln, NE), and polyclonal (rabbit) anticathepsin D was from Calbaiochem (San Diego, CA). Transferrin labeled with Oregon green was purchased from Molecular Probes (Eugene, OR).

Custom-made synthesis of 5-carboxytetramethylrhodamine (TAMRA) labeled peptides was performed by SBS Genetech (China). According to certificate of analysis provided by the manufacturer, purity of the peptides for TAMRA-NLS was 98.94%, and that for the TAMR-decoy peptide was >90% as assessed by HPLC and mass spectrometry. pEYFP pECFP plasmids were obtained from Clonetech (Mountain View, CA), and pcDNA3.1 plasmids containing wild-type or G93A mutant hSOD1 cDNA were kindly provided by Dr. David Gozal.

Cell Cultures. NSC-34 cells, kindly donated by Dr. Neil Cashman, were grown in DMEM supplemented with 5% heat inactivated FCS, 1 mM glutamine, and antibiotics (100 μg/mL penicillin and 100 μg/mL streptomycin) at 37 °C in a 5% CO_2 humidified atmosphere. NSC-34 cell lines expressing the inducible forms of WThSOD1 or G93AhSOD1 fused with the green fluorescence protein (GFP) were prepared essentially as described[7] and kept in selection by addition of G418 (700 μg/mL) plus hygromycin B (200 μg/mL) until used. The cells were incubated with doxycycline (1 μg/mL, 24 h) to induce WThSOD1-GFP and G93AhSOD1-GFP proteins expression.

Myc Tagged MDH1 Fragments Library. MDH1 cDNA was digested with AluI and DpnI to yield 30 different peptides. PEYFP f1 f2 f3 plasmids were prepared as described[7] and digested with AgeI and HindIII. Homologue oligonucleotide sequences containing kozak ATG and the myc tag with AgeI/HindIII edges, (sense sequence) 5′CCGGTCGCCACCATGGAGCAGAAGCTCATAAGTGAGGAAGACTTGA3′ and (antisense sequence) 5′AGCTTCAAGTCTTCCTCACTTATGGAGCTTCTGCTCCATGGTGGCGA3′, were annealed and ligated into the digested plasmid to yield the myc-tag expressing plasmids set pEmyc f1, f2 f3 containing three different reading frames in order to ensure expression of the peptide sequences. MDH1 fragments were cloned into the EcoRV site in the pEmyc f1, f2 f3 plasmids set. The library containing 180 different clones (30 fragments each in three frames and two orientations) was amplified in DH5α bacteria for 12 h in 37 °C on LB agar plates containing kanamycin.

FRET Based Screening in Live Cells. pECFP-G93AhSOD1 and pEYFP-MDH1 expression plasmids were prepared as described[7] and co-transfected into NSC-34 cells together with the myc tagged MDH1 fragments library. Cells were washed with PBS after 48 h and harvested. CFP tagged cells that showed no FRET signal were sorted out using a cell sorter (FACS) with 425 nm excitation laser and a 525/540 nm emission filter. A population that was present only in cells co-transfected with the pECFP-G93AhSOD1 and pEYFP-MDH1 plasmids was defined as a positive FRET population.[7] To determine the FRET negative gating area, FACS analysis was performed in NSC-34 cells transfected with pECFP-G93AhSOD1 expressing plasmid. The FACS gating area was thus set on the population defined by a negative FRET signal (see Results). RNA was extracted from the sorted cells, converted into cDNA, and subjected to PCR amplification and sequencing. The DNA sequence from the sorted cells was recloned. The identified clones were reanalyzed in the FACS based system to verify their ability to compete for the G93AhSOD1−MDH1 interaction.

RNA Preparation and Clone Analysis. Sorted cells were used for RNA extraction and subsequent preparation of cDNA, cloning, and sequencing. Total RNA was extracted from FRET negative cells and subjected to reverse transcription using EZ-first strand cDNA synthesis RNA kit followed by PCR amplification with the following primers: forward 5′ GCTACCGGTCGCCACCATGGAGCAGAAGC, reverse 5′ GGACAAACCACAACTAGAATGCAG 3′. PCR product was digested with HindIII and BamHI and cloned into a pEmyc f1 plasmid (as the digested peptide sequence already contains the frame that was expressed in the screening). The 32 individual clones were analyzed by PCR using the same primers as above to evaluate clone sizes. Representative numbers of clones from each size were sequenced (Table1).

Pull-Down Immunoprecipitation. NSC-34 cells were co-transfected with pCDNA3.1-WThSOD1 and pEYFP-MDH1 or with pCDNA3.1-G93AhSOD1 and pEYFP-MDH1. The medium was replenished 24 h later with fresh medium containing 1 μM of the potential interaction impairing peptide, a control (NLS) peptide, or vehicle (0.02% acetic acid). After 48 h cells were lysed in solubilization buffer (50 mM Hepes, pH 7.5, 150 mM NaCl, 10% glycerol, 1% Triton-X, 1 mM EDTA, 1 mM EGTA, and 1.5 mM $MgCl_2$). Samples containing 0.5 mg of protein were subjected to immunoprecipitation using anti-hSOD1 antibodies immobilized on protein A-coupled Sepharose beads. Immunoprecipitated proteins were analyzed by Western blots using polyclonal (rabbit) anti-hSOD1 as a primary and IRDey-800-linked antirabbit IgG as secondary antibodies. Analysis was performed in Odyssey fluorescence reader (Li-Cor Bioscience).

Molecular Docking Based Analysis of the SOD1−MDH1 Complex. The Patchdock molecular docking algorithm based on shape complementarity principles was applied to assess the possibility that the decoy peptide sequence is located in MDH1 in a position comprising the G93AhSOD1/MDH1 interacting motif. We first studied the interaction between the crystal structure of MDH1 (PDB code 5MDH) with that of the FALS-associated human copper−zinc superoxide dismutase (CuZnSOD) mutant D125H (PDB code 1p1v).

Methylene Blue Cell Viability Assay. Media were discarded, and an amount of 80 μL of 4% paraformaldehyde/well in a 96-well plate was added for 2 h. Cells were then washed with 100 μL/well of 0.1 M sodium borate buffer, pH 8.5, and then incubated with 80 μL of 1% methylene blue solution for 20 min. Excess dye was washed away extensively. The residual methylene blue was eluted from the cells with 200 μL/well of 0.1 M HCl, and optical density was read in the ELISA plate reader in at 595 nM.

Rotenone Toxicity Assay. WThSOD1-GFP and G93AhSOD1-GFP cells were plated in a 96-well plate (1.5× 104 cells/well)

and incubated with doxycycline in DMEM containing 5% FCS for 24 h. The medium was then replaced with 5% DMEM containing 2 μM rotenone or vehicle and the tested TAMRA labeled peptides (1 μM in 0.02% acetic acid) or vehicle (0.02% acetic acid). Cell viability was assessed 24 h later using the methylene blue assay ($N = 10$). Results were presented as % of survival of rotenone treated cells of vehicle treated control ($N = 5-8$ different experiments).

Low Glucose Assay. WThSOD1-GFP and G93AhSOD1-GFP cells were plated in a 96-well plate (1.5 × 104 cells/well) and incubated with doxycycline in DMEM containing 5% FCS for 24 h. The medium was then replaced with 5% DMEM containing low (2 mg/mL) or normal (4.5 mg/mL) glucose with vehicle (0.02% acetic acid) or with 5% DMEM containing 2 mg/mL glucose or control DMEM containing 4.5 mg/mL glucose with decoy-TAMRA labeled peptides (1 μM) . Cell viability was assessed 48 h later using the methylene blue assay ($N = 10$). Results were presented as % of survival of cells with or without the peptide in the presence of 2 mg/mL glucose of that with 4.5 mg/mL glucose ($N = 4$).

ATP Assessments. WThSOD1-GFP and G93AhSOD1-GFP cells were plated in a 96-well plate (1.5 × 104 cells/well) and incubated with doxycycline in DMEM containing 5% FCS for 24 h. The medium was then replaced with 5% DMEM containing 1 μM of the TAMRA labeled decoy or NLS peptides. ATP content was evaluated 48 h later using the ATP assay kit according to the manufacturer's instructions.

TAMRA Peptide Localization Studies. NSC-34 cells (6×10^5) were plated on a 22 mm^2 cover glass and grown for 24 h. For G93AhSOD1 colocalization studies, cells were transfected with G93AhSOD1-CFP expression plasmid and, 24 h later, incubated with 1 μM TAMRA labeled peptide for 24 h and fixed with 4% paraformaldehyde. For mitochondrial colocalization studies cells were incubated with 1 μM TAMRA labeled peptide for 24 h and then incubated with 0.5 mg/mL MTT for 30 min at 37 °C and washed with PBS. For lysosomal colocalization studies cells were incubated with 1 μM TAMRA labeled peptide for 24 h and then fixed with 4% paraformaldehyde. Fixed cells were incubated with anti cathepsin-D or anti-Lamp1 as lysosomes markers. For early endosomes colocalization studies, cells were transfected with RUB5-GFP expression plasmid and 24 h later incubated with 1 μM TAMRA labeled peptide for 24 h and fixed with 4% paraformaldehyde. For endosomes colocalization studies Oregon green labeled transferrin was added to the NSC-34 peptide labeled cells for 30 min at 37 °C and the cells were then fixed with 4% paraformaldehyde. All colocalization analyses were performed using a Zeiss LSM510 confocal microscope.

Acknowledgment. The study was supported by an ISF Morasha grant. Y.M. was supported in part by the Gimmelfarb foundation. N.Z. is an incumbent of the Michael Gluck Chair of Neuropharmacology and ALS Research.

References

(1) Carrì, M. T.; Ferri, A; Battistoni, A; Famhy, L; Gabbianelli, R; Poccia, F; Rotilio, G. Expression of a Cu,Zn superoxide dismutase typical of familial amyotrophic lateral sclerosis induces mitochondrial alteration and increase of cytosolic Ca^{2+} concentration in transfected neuroblastoma SH-SY5Y cells. *FEBS Lett*. **1997**, *414*, 365–368.
(2) Kruman, I. I.; Pedersen, W. A.; Springer, J. E.; Mattson, M. P. ALS-linked Cu/Zn-SOD mutation increases vulnerability of motor neurons to excitotoxicity by a mechanism involving increased oxidative stress and perturbed calcium homeostasis. *Exp. Neurol*. **1999**, *160*, 28–39.
(3) Beal, M. F. Mitochondria and the pathogenesis of ALS. *Brain* **2000**, *123* (Part 7), 1291–1292.
(4) Menzies, F. M.; Cookson, M. R.; Taylor, R. W.; Turnbull, D. M.; Chrzanowska-Lightowlers, Z. M.; Dong, L; Figlewicz, D. A.; Shaw, P. J. Mitochondrial dysfunction in a cell culture model of familial amyotrophic lateral sclerosis. *Brain* **2002**, *125*, 1522–1533.
(5) Bendotti, C.; Carri, M. T. Lessons from models of SOD1-linked familial ALS. *Trends Mol. Med*. **2004**, *10*, 393–400.
(6) Rizzardini, M; Mangolini, A; Lupi, M; Ubezio, P; Bendotti, C; Cantoni, L. Low levels of ALS-linked Cu/Zn superoxide dismutase increase the production of reactive oxygen species and cause mitochondrial damage and death in motor neuron-like cells. *J. Neurol. Sci*. **2005**, *232*, 95–103.
(7) Mali, Y.; Zisapels, N. Gain of interaction of ALS-linked G93A superoxide dismutase with cytosolic malate dehydrogenase. *Neurobiol. Dis*. **2008**, *32*, 133–141.
(8) Watanabe, Y; Morita, E; Fukada, Y; Doi, K; Yasui, K; Kitayama, M; Nakano, T; Nakashima, K. Adherent monomer-misfolded SOD1. *PLoS One* **2008**, *3*, e3497.
(9) McKenna, M. C.; Waagepetersen, H. S.; Schousboe, A.; Sonnewald, U. Neuronal and astrocytic shuttle mechanisms for cytosolic-mitochondrial transfer of reducing equivalents: current evidence and pharmacological tools. *Biochem. Pharmacol*. **2006**, *71*, 399–407.
(10) Rizzardini, M; Lupi, M; Mangolini, A; Babetto, E; Ubezio, P; Cantoni, L. Neurodegeneration induced by complex I inhibition in a cellular model of familial amyotrophic lateral sclerosis. *Brain Res. Bull*. **2006**, *69*, 465–474.
(11) Beretta, S; Sala, G; Mattavelli, L; Ceresa, C; Casciati, A; Ferri, A; Carrì, M. T.; Ferrarese, C. Mitochondrial dysfunction due to mutant copper/zinc superoxide dismutase associated with amyotrophic lateral sclerosis is reversed by *N*-acetylcysteine. *Neurobiol. Dis*. **2003**, *13*, 213–221.
(12) Chan, F. K. Monitoring molecular interactions in living cells using flow cytometric analysis of fluorescence resonance energy transfer. *Methods Mol. Biol*. **2004**, *261*, 371–382.
(13) Trejo, F; Gelpí, J. L.; Ferrer, A; Boronat, A; Busquets, M; Cortés, A. Contribution of engineered electrostatic interactions to the stability of cytosolic malate dehydrogenase. *Protein Eng*. **2001**, *14*, 911–917.
(14) Barron, J. T.; Gu, L.; Parrillo, J. E. Malate-aspartate shuttle, cytoplasmic NADH redox potential, and energetics in vascular smooth muscle. *J. Mol. Cell. Cardiol*. **1998**, *30*, 1571–1579.
(15) Browne, S. E.; Yang, L; DiMauro, J. P.; Fuller, S. W.; Licata, S. C.; Beal, M. F. Bioenergetic abnormalities in discrete cerebral motor pathways presage spinal cord pathology in the G93A SOD1 mouse model of ALS. *Neurobiol. Dis*. **2006**, *22*, 599–610.
(16) Jung, C.; Higgins, C. M.; Xu, Z. A quantitative histochemical assay for activities of mitochondrial electron transport chain complexes in mouse spinal cord sections. *J. Neurosci. Methods* **2002**, *114*, 165–172.
(17) Jung, C.; Higgins, C. M.; Xu, Z. Mitochondrial electron transport chain complex dysfunction in a transgenic mouse model for amyotrophic lateral sclerosis. *J. Neurochem*. **2002**, *83*, 535–545.
(18) Mattiazzi, M; D'Aurelio, M; Gajewski, C. D.; Martushova, K; Kiaei, M; Beal, M. F.; Manfredi, G. Mutated human SOD1 causes dysfunction of oxidative phosphorylation in mitochondria of transgenic mice. *J. Biol. Chem*. **2002**, *277*, 29626–29633.
(19) Bogliolo, M.; Borghini, S.; Abbondandolo, A.; Degan, P. Alternative metabolic pathways for energy supply and resistance to apoptosis in Fanconi anaemia. *Mutagenesis* **2002**, *17*, 25–30.